NACA RM L57J25a

NACA

RESEARCH MEMORANDUM

INVESTIGATION OF THE AERODYNAMIC CHARACTERISTICS IN PITCH AND SIDESLIP OF A 45° SWEPT-WING AIRPLANE CONFIGURATION WITH VARIOUS VERTICAL LOCATIONS OF THE WING AND HORIZONTAL TAIL

STATIC LATERAL AND DIRECTIONAL STABILITY; MACH NUMBERS OF 1.41 AND 2.01

By M. Leroy Spearman and Ross B. Robinson

Langley Aeronautical Laboratory
Langley Field, Va.

NATIONAL ADVISORY COMMITTEE FOR AERONAUTICS

WASHINGTON

December 27, 1957

Declassified May 29, 1959

NATIONAL ADVISORY COMMITTEE FOR AERONAUTICS

RESEARCH MEMORANDUM

INVESTIGATION OF THE AERODYNAMIC CHARACTERISTICS IN PITCH AND SIDESLIP OF A 45° SWEPT-WING AIRPLANE CONFIGURATION WITH VARIOUS VERTICAL LOCATIONS OF THE WING AND HORIZONTAL TAIL

STATIC LATERAL AND DIRECTIONAL STABILITY; MACH NUMBERS OF 1.41 AND 2.01

By M. Leroy Spearman and Ross B. Robinson

SUMMARY

An investigation has been conducted in the Langley 4- by 4-foot supersonic pressure tunnel to determine the effects of wing and horizontal-tail vertical location on the aerodynamic characteristics in sideslip at various angles of attack for a supersonic airplane configuration at Mach numbers of 1.41 and 2.01. The basic model was equipped with a wing and horizontal tail, each having 45° sweep and an aspect ratio of 4. The wing had a taper ratio of 0.2 and NACA 65A004 sections; the horizontal tail had a taper ratio of 0.4 and NACA 65A006 sections.

The configurations investigated included a high-wing, a midwing, and a low-wing arrangement, and four different horizontal-tail locations varying from a position 0.208 semispan below to 0.556 semispan above the body center line. Tests were made with the horizontal tail on and off, the vertical tail on and off, and with the wing both on and off. In addition, the midwing configuration with horizontal tail off was tested with a series of vertical tails having quarter-chord-line sweeps of 10.8°, 35°, 47°, and 60°.

The results indicated that the directional stability in the Mach number range from 1.4 to 2.0 was higher for the low-wing configuration and lower for the high-wing configuration as a result, primarily, of the induced sidewash effects on the afterbody and tail. The use of the high wing provided a positive dihedral effect whereas the use of the low wing provided a negative dihedral effect. In general, the effects of wing position on directional stability and effective dihedral were similar to those that occur at subsonic speeds.

INTRODUCTION

The experimentally determined effects of wing and tail position on the aerodynamic characteristics of generalized aircraft configurations can be of considerable usefulness to the designer in the estimation of the stability and performance of similar specific configurations. In addition, such generalized results may be useful in the evaluation of various calculative methods for the prediction of the aerodynamic characteristics of airplanes. A considerable amount of such experimental data is available at low speeds (refs. 1 to 4, for example) wherein the influence of both plan form and position of wings and tails has been determined from wind-tunnel tests of models simulating high-speed aircraft. Similar investigations have been extended to high subsonic Mach numbers (for example, refs. 5 to 9) and some results concerning the effects of tail and wing location on the longitudinal and lateral characteristics of some rocket-propelled models have been obtained through the transonic speed range (refs. 10 to 12). A limited amount of such experimental data is available in the supersonic speed range. One example is the investigation reported in reference 13 in which the effects of wing vertical location on the longitudinal characteristics of wing-body combinations were determined in the Mach number range from 0.61 to 0.91 and from 1.20 to 1.90.

In order to provide additional results of general interest to the designer for the supersonic speed range, an investigation has been conducted in the Langley 4- by 4-foot supersonic pressure tunnel at Mach numbers of 1.41 and 2.01 to determine the effects of wing vertical location and horizontal-tail vertical location on the longitudinal and lateral aerodynamic characteristics of a complete model having a 45° swept wing and tail. The basic results, without analysis, are presented for a Mach number of 2.01 in reference 14. An analysis of the effects of wing vertical location and geometric dihedral for the wing-body combination at a Mach number of 2.01 is presented in reference 15. The static longitudinal stability and control characteristics at a Mach number of 2.01 for the high-wing, midwing, and low-wing configurations, each with four different vertical positions of the horizontal tail, are presented in reference 16. This paper presents the static lateral and directional stability characteristics at Mach numbers of 1.41 and 2.01 for various wing and tail arrangements.

SYMBOLS

The results are presented as coefficients of forces and moments referred to the body axes system (fig. 1) with the reference center of

moments located at 25 percent of the wing mean geometric chord. The symbols are defined as follows:

C_Y	lateral-force coefficient, $\frac{F_Y}{qS}$
C_l	rolling-moment coefficient, $\frac{M_X}{qSb}$
C_n	yawing-moment coefficient, $\frac{M_Z}{qSb}$
F_Y	force along Y-axis
M_X	moment about X-axis
M_Z	moment about Z-axis
q	free-stream dynamic pressure
S	wing area including body intercept
S_v	exposed area of vertical tail
b	wing span
c	chord
$\bar{c}$	wing mean geometric chord
α	angle of attack, deg
β	angle of sideslip, deg
Λ	angle of sweep, deg
λ	taper ratio
A	aspect ratio
M	Mach number
C_{n_β}	directional stability derivative
C_{l_β}	effective dihedral derivative

C_{Y_β} lateral-force derivative

Designation of airplane components:

B body

W wing

V vertical tail

H horizontal tail

Subscripts:

H high

L low

MODEL AND APPARATUS

A drawing of the model is shown in figure 2(a) and the geometric characteristics of the model are presented in table I.

The model fuselage was a body of revolution having a length-diameter ratio of about 11 and was composed of a 3.5-caliber ogive nose, a cylindrical midsection, and a slightly boattail rear section. The fuselage coordinates are given in table II. The wing had a quarter-chord-line sweep of 45°, an aspect ratio of 4, a taper ratio of 0.2, and NACA 65A004 sections in the stream direction. The horizontal tail had a quarter-chord-line sweep of 45°, an aspect ratio of 4, a taper ratio of 0.6, and NACA 65A006 sections in the stream direction. The model was equipped with a vertical tail with relatively thick slab-type sections to facilitate mounting of the horizontal tail and a small ventral fin. The position of the horizontal tail was variable from a point below the body on the ventral fin (0.208b/2 below body center line; designated tail position number 4) to three positions above the body on the vertical tail (0.208b/2, 0.382b/2, and 0.556b/2 above body center line; designated as tail positions 3, 2, and 1, respectively). The uppermost location (tail position 1) was atop the vertical tail and corresponded to a T-tail arrangement. A series of swept vertical tails having hexagonal sections was also provided. (See fig. 2(b).) The model was designed so that the wing could be located in a low, middle, or high position. The dihedral and incidence angles of the wing and horizontal tail were zero.

Force measurements were made through the use of a six-component internal strain-gage balance. The tests were made in the Langley 4- by 4-foot supersonic pressure tunnel which is described in reference 17.

TESTS, CORRECTIONS, AND ACCURACY

The conditions for the tests were:

Mach number	1.41	2.01
Stagnation temperature, $^{\circ}F$	100	110
Stagnation pressure, lb/sq in. abs	10	12
Reynolds number based on $\bar{c}$	1.72×10^6	1.66×10^6

The stagnation dewpoint was maintained sufficiently low (-25° F or less) so that no condensation effects were encountered in the test section.

The sting angle was corrected for the deflection under load. The Mach number variation in the test section was approximately ± 0.01 and the flow-angle variation in the vertical and horizontal planes did not exceed about $\pm 0.1^{\circ}$.

The estimated errors in the individual measured quantities are as follows:

C_Y	± 0.001
C_n	± 0.0005
C_l	± 0.0004
β, deg	± 0.2
α, deg	± 0.2

DISCUSSION

The variations of C_n, C_l, and C_Y with angle of sideslip at angles of attack of approximately 0° and 15.3° for various configurations at $M = 1.41$ are shown in figures 3 to 5. These figures which are typical of the data obtained serve to indicate the linearity of the results. Variations of the sideslip derivatives C_{n_β}, C_{l_β}, and C_{Y_β} throughout the angle-of-attack range for $M = 1.41$ were then determined with the increments obtained from tests in which the sideslip angle was held constant at 0° and 4° while the angle of attack was varied.

The sideslip derivatives for the basic model at $M = 2.01$ were obtained from reference 14, the necessary conversions being made from the stability-axes system to the body-axes system.

Effects of Wing Position

Directional stability.- The effects of wing position on the directional characteristics throughout the angle-of-attack range for various model configurations are presented in figure 6 for $M = 1.41$ and 2.01. In general, the directional stability derivative C_{n_β} with the tail on is highest for the low-wing configuration and lowest for the high-wing configuration at both Mach numbers. At the higher angles of attack, C_{n_β} decreases for each wing position. With the vertical tail off, an opposite effect occurs in that the level of instability at angle of attack is less for the high wing and greater for the low wing. These effects are similar to those that occur at subsonic speeds. (See ref. 1.)

These characteristics apparently result in part from the sidewash disturbance caused by the wing-body juncture. This sidewash, as pointed out in reference 1, results from the differential wing pressures near the wing root that are created by the lateral component of velocity due to sideslip. For the high-wing case this sidewash is adverse above and favorable below the center of the wing wake. The reverse is true for the low-wing case. Hence, at zero angle of attack, the afterbody lies in the same type of flow region for either wing position and the values of C_{n_β} for the tail-off configurations are essentially unchanged by wing position. With increasing angle of attack, the low-wing arrangement becomes increasingly unstable since the afterbody moves down through a region of adverse sidewash. For the high-wing arrangement, there is some reduction in the instability with increasing angle of attack as the afterbody moves down through a region of favorable sidewash and into an undisturbed flow region.

With the addition of the vertical tail at $\alpha = 0^\circ$, each configuration becomes stable at both Mach numbers. However, the tail contribution to C_{Y_β} and C_{n_β} is less with the high wing since this arrangement places the tail in a region of adverse sidewash. With increasing angle of attack, the tail contribution continues to decrease for the high-wing arrangement as the tail passes through the region of adverse sidewash. For the low-wing arrangement, there is some increase in tail contribution with increasing angle of attack as the tail passes through a region of favorable sidewash.

There is relatively little change in C_{n_β} with angle of attack for the midwing and wing-off configurations with the tail removed except at the higher angles of attack at $M = 2.01$. This result might be expected since at the lower angles of attack these arrangements are essentially symmetric whereas at the higher angles of attack there is a possibility of asymmetric vorticity appearing in the body flow field.

The midwing and wing-off configurations become stable when the vertical tail is added. However, with increasing angle of attack, the tail contributions to C_{Y_β} and C_{n_β} for these configurations also decrease and, in fact, the wing-off model at $M = 2.01$ becomes directionally unstable. This result is an indication of the effect of forebody vorticity on the tail contribution. This effect is also present for the wing-on cases and the resultant directional characteristics are caused by a combination of the forebody vorticity and the wing-body induced disturbance. It is interesting to note that, for the tail-on configurations at the higher angles of attack for $M = 2.01$, the addition of the wing resulted in higher stability than that obtained for the wing-off case. The fact that this was true even for the high-wing arrangement, which in itself provides a destabilizing sidewash at the tail, indicates that the position and possibly the existence of the forebody vortex is affected by the presence of the high wing.

It might be pointed out that, in addition to the expected difference in level in C_{n_β} and C_{Y_β} between $M = 1.41$ and 2.01, the effects of wing height appear to be less at the higher Mach number. This condition may result in part from a reduction in vortex strength for the wing-body induced flows as the wing lift-curve slope decreases. However, the decrease in wing-height effects at $M = 2.01$ might also be expected because of the lower tail lift-curve slope which, even for a constant sidewash angle at the tail, would result in a smaller incremental change in tail contribution.

An additional effect to consider is the change with angle of attack of the dynamic pressure in the wing flow field. This change involves an increase in dynamic pressure below the wing and a decrease in dynamic pressure above the wing for positive angles of attack. The effects of these changes are relatively small up to $M \approx 2$. Above $M \approx 2$, however, the dynamic-pressure changes become large and, when coupled with the fact that the wing Mach lines are swept back more nearly over the afterbody and tail, may outweigh the effects of vorticity.

Effective dihedral.- For both Mach numbers the effect of wing position on the rolling-moment characteristics is to increase the dihedral effect $(-C_{l_\beta})$ for the high wing and to reduce the dihedral effect for the low wing with the vertical tail on or off. (See fig. 6.) This change in

dihedral effect is similar to that which occurs at low speeds (ref. 1) and is a result of the lateral component of velocity about the yawed body which induces a positive lift for the leading wing and a negative lift for the trailing wing for the high-wing arrangement whereas the opposite effect occurs for the low-wing arrangement.

Effect of Horizontal-Tail Position

Directional stability.- The effects of horizontal-tail position on C_{n_β} at $M = 1.41$ and 2.01 are relatively small. (See fig. 7.) In general, the addition of the horizontal tail in any position at zero incidence results in some increase in C_{n_β} because of the end-plate effect on the vertical tail. However, as pointed out in reference 18, when the horizontal tail is deflected in a direction to provide longitudinal trim (trailing edge up), the result is an increase in C_{n_β} for the low tail and a decrease in C_{n_β} for the high tail.

Effective dihedral.- The addition of the horizontal tail has a significant effect on C_{l_β} (fig. 7) wherein the low tail provides a reduction in dihedral effect and the high tail provides an increase in dihedral effect at both Mach numbers for all wing positions. This trend is consistent with that to be expected from the interference effects of the horizontal tail on the vertical tail. The effectiveness of the ventral fin is increased by the presence of the low horizontal tail so that an increment of negative dihedral effect is provided. With the higher tails, the effectiveness of the upper vertical tail is increased so that an increment of positive dihedral effect is provided.

Effects of Vertical-Tail Sweep

The effects of vertical-tail sweepback on the sideslip derivatives of the midwing configuration with the horizontal tail off at $M = 1.41$ and 2.01 are shown in figure 8. In general, the moderately swept (35° and 47°) tails appear to provide slightly better directional characteristics than either the 10.8° or 60° swept tails. These results are dependent upon various interrelated effects that accompany such tail modifications. The change in lift-curve slope of the tail with increasing sweepback is fairly small. However, with increasing sweepback the effective moment arm of the tail increases while the carryover lateral-force interference effect between the body and the tail decreases. The maximum benefits of the effective tail moment arm and of the interference effects appear to occur at the moderate sweeps.

Effect of Ventral Fin

The effect of the ventral fin on the sideslip derivatives at $M = 2.01$ for the midwing model with the horizontal tail off are shown in figure 9. The ventral fin provides an increase in lateral force and directional stability that is relatively unaffected by increasing the angle of attack since the ventral fin is located in an essentially undisturbed region of flow.

CONCLUSIONS

The results of an investigation of the static lateral and directional stability characteristics of a 45° swept-wing airplane configuration at Mach numbers of 1.41 and 2.01 indicated the following conclusions:

1. In general, the directional stability is higher for the low-wing configurations and lower for the high-wing configurations at both Mach numbers as a result, primarily, of the induced sidewash effects on the afterbody and tail.

2. The use of the high wing provided a positive dihedral effect whereas the use of the low wing provided a negative dihedral effect for the configuration either with or without the vertical tail.

3. In general, the effects of wing position on the directional stability and effective dihedral were the same as those that occur at subsonic speeds.

Langley Aeronautical Laboratory,
National Advisory Committee for Aeronautics,
Langley Field, Va., October 7, 1957.

REFERENCES

1. Goodman, Alex: Effects of Wing Position and Horizontal-Tail Position on the Static Stability Characteristics of Models With Unswept and 45° Sweptback Surfaces With Some Reference to Mutual Interference. NACA TN 2504, 1951.

2. Brewer, Jack D., and Lichtenstein, Jacob H.: Effect of Horizontal Tail on Low-Speed Static Lateral Stability Characteristics of a Model Having 45° Sweptback Wing and Tail Surfaces. NACA TN 2010, 1950.

3. Queijo, M. J., and Wolhart, Walter D.: Experimental Investigation of the Effect of Vertical-Tail Size and Length and of Fuselage Shape and Length on the Static Lateral Stability Characteristics of a Model With 45° Sweptback Wing and Tail Surfaces. NACA Rep. 1049, 1951. (Supersedes NACA TN 2168.)

4. Goodman, Alex, and Thomas, David F., Jr.: Effects of Wing Position and Fuselage Size on the Low-Speed Static and Rolling Stability Characteristics of a Delta-Wing Model. NACA Rep. 1224, 1955. (Supersedes NACA TN 3063.)

5. Wiggins, James W., Kuhn, Richard E., and Fournier, Paul G.: Wind-Tunnel Investigation To Determine the Horizontal- and Vertical-Tail Contributions to the Static Lateral Stability Characteristics of a Complete-Model Swept-Wing Configuration at High Subsonic Speeds. NACA TN 3818, 1956. (Supersedes NACA RM L53E19.)

6. Morrison, William D., Jr., and Alford, William J., Jr.: Effects of Horizontal-Tail Position and a Wing Leading-Edge Modification Consisting of a Full-Span Flap and a Partial-Span Chord-Extension on the Aerodynamic Characteristics in Pitch at High Subsonic Speeds of a Model With a 45° Sweptback Wing. NACA TN 3952, 1957. (Supersedes NACA RM L53E06.)

7. Alford, William J., Jr., and Pasteur, Thomas B., Jr.: The Effects of Changes in Aspect Ratio and Tail Height on the Longitudinal Stability Characteristics at High Subsonic Speeds of a Model With a Wing Having 32.6° Sweepback. NACA RM L53L09, 1954.

8. Goodson, Kenneth W., and Becht, Robert E.: Wind-Tunnel Investigation at High Subsonic Speeds of the Stability Characteristics of a Complete Model Having Sweptback-, M-, W-, and Cranked-Wing Plan Forms and Several Horizontal-Tail Locations. NACA RM L54C29, 1954.

9. Few, Albert G., Jr., and King, Thomas J., Jr.: Some Effects of Tail Height and Wing Plan Form on the Static Longitudinal Stability Characteristics of a Small-Scale Model at High Subsonic Speeds. NACA TN 3957, 1957. (Supersedes NACA RM L54G12.)

10. Parks, James H., and Kehlet, Alan B.: Longitudinal Stability, Trim, and Drag Characteristics of a Rocket-Propelled Model of an Airplane Configuration Having a 45° Sweptback Wing and an Unswept Horizontal Tail. NACA RM L52F05, 1952.

11. Parks, James H., and Kehlet, Alan B.: Longitudinal Stability and Trim of Two Rocket-Propelled Airplane Models Having 45° Sweptback Wings and Tails With the Horizontal Tail Mounted in Two Positions. NACA RM L53J12a, 1953.

12. Gillis, Clarence L., and Chapman, Rowe, Jr.: Effect of Wing Height and Dihedral on the Lateral Stability Characteristics at Low Lift of a 45° Swept-Wing Airplane Configuration As Obtained From Time-Vector Analyses of Rocket-Propelled-Model Flights at Mach Numbers From 0.7 to 1.3. NACA RM L56E17, 1956.

13. Heitmeyer, John C.: Effect of Vertical Position of the Wing on the Aerodynamic Characteristics of Three Wing-Body Combinations. NACA RM A52L15a, 1953.

14. Spearman, M. Leroy, Driver, Cornelius, and Hughes, William C.: Investigation of Aerodynamic Characteristics in Pitch and Sideslip of a 45° Sweptback-Wing Airplane Model With Various Vertical Locations of Wing and Horizontal Tail - Basic-Data Presentation, M = 2.01. NACA RM L54L06, 1955.

15. Spearman, M. Leroy: Investigation of the Aerodynamic Characteristics in Pitch and Sideslip of a 45° Sweptback-Wing Airplane Model With Various Vertical Locations of the Wing and Horizontal Tail - Effect of Wing Location and Geometric Dihedral for the Wing-Body Combination, M = 2.01. NACA RM L55B18, 1955.

16. Spearman, M. Leroy, and Driver, Cornelius: Investigation of Aerodynamic Characteristics in Pitch and Sideslip of a 45° Sweptback-Wing Airplane Model With Various Vertical Locations of Wing and Horizontal Tail - Static Longitudinal Stability and Control, M = 2.01. NACA RM L55L06, 1956.

17. Robinson, Ross B., and Driver, Cornelius: Aerodynamic Characteristics at Supersonic Speeds of a Series of Wing-Body Combinations Having Cambered Wings With an Aspect Ratio of 3.5 and a Taper Ratio of 0.2 - Effects of Sweep Angle and Thickness Ratio on the Aerodynamic Characteristics in Pitch at M = 1.60. NACA RM L51K16a, 1952.

18. Spearman, M. Leroy: Some Factors Affecting the Static Longitudinal and Directional Stability Characteristics of Supersonic Aircraft Configurations. NACA RM L57E24a, 1957.

TABLE I.- GEOMETRIC CHARACTERISTICS OF MODEL

Wing:	
Area, sq in.	144
Span, in.	24
Root chord, in.	10
Tip chord, in.	2
Taper ratio	0.2
Aspect ratio	4
Mean geometric chord, in.	6.89
Spanwise location of mean geometric chord, percent wing semispan	38.9
Incidence, deg	0
Sweep of quarter-chord line, deg	45
Airfoil section	NACA 65A004
Horizontal tail:	
Area, sq in.	28.6
Span, in.	10.73
Root chord, in.	3.353
Tip chord, in.	2.012
Taper ratio	0.6
Aspect ratio	4
Sweep of quarter-chord line, deg	45
Airfoil section	NACA 65A006
Basic vertical tail (excluding ventral fin):	
Area to body center line, sq in.	43.5
Span from body center line, in.	7.48
Root chord at body center line, in.	8.17
Tip chord, in.	3.44
Taper ratio	0.42
Aspect ratio	1.29
Sweep of leading edge, deg	35
Airfoil section	Wedge nose, slab sides with constant thickness of 0.437 inch
Ventral fin:	
Exposed area, sq in.	8.54
Tip chord, in.	3.25
Sweep of leading edge, deg	70.1
Body:	
Length, in.	36.50
Diameter (maximum), in.	3.33
Diameter (base), in.	2.67
Length-diameter ratio	10.96

TABLE II.- FUSELAGE COORDINATES

Longitudinal station, in.	Radius, in.
0	0
2.000	.530
4.000	.956
6.000	1.280
8.000	1.506
10.000	1.634
11.667	1.667
27.750	1.667
36.500	1.344

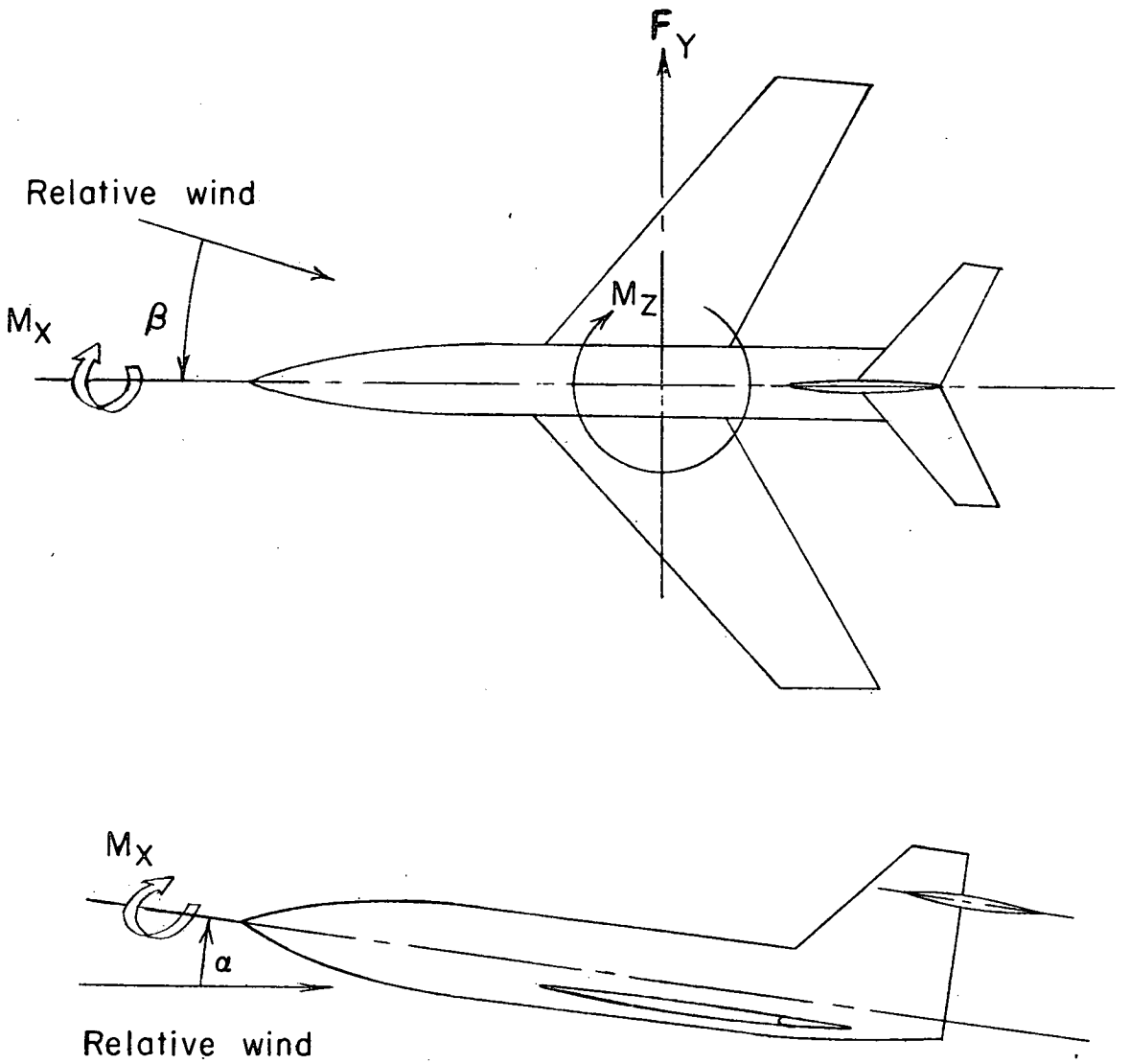

Figure 1.- Body axis system. Arrows indicate positive directions of forces and moments.

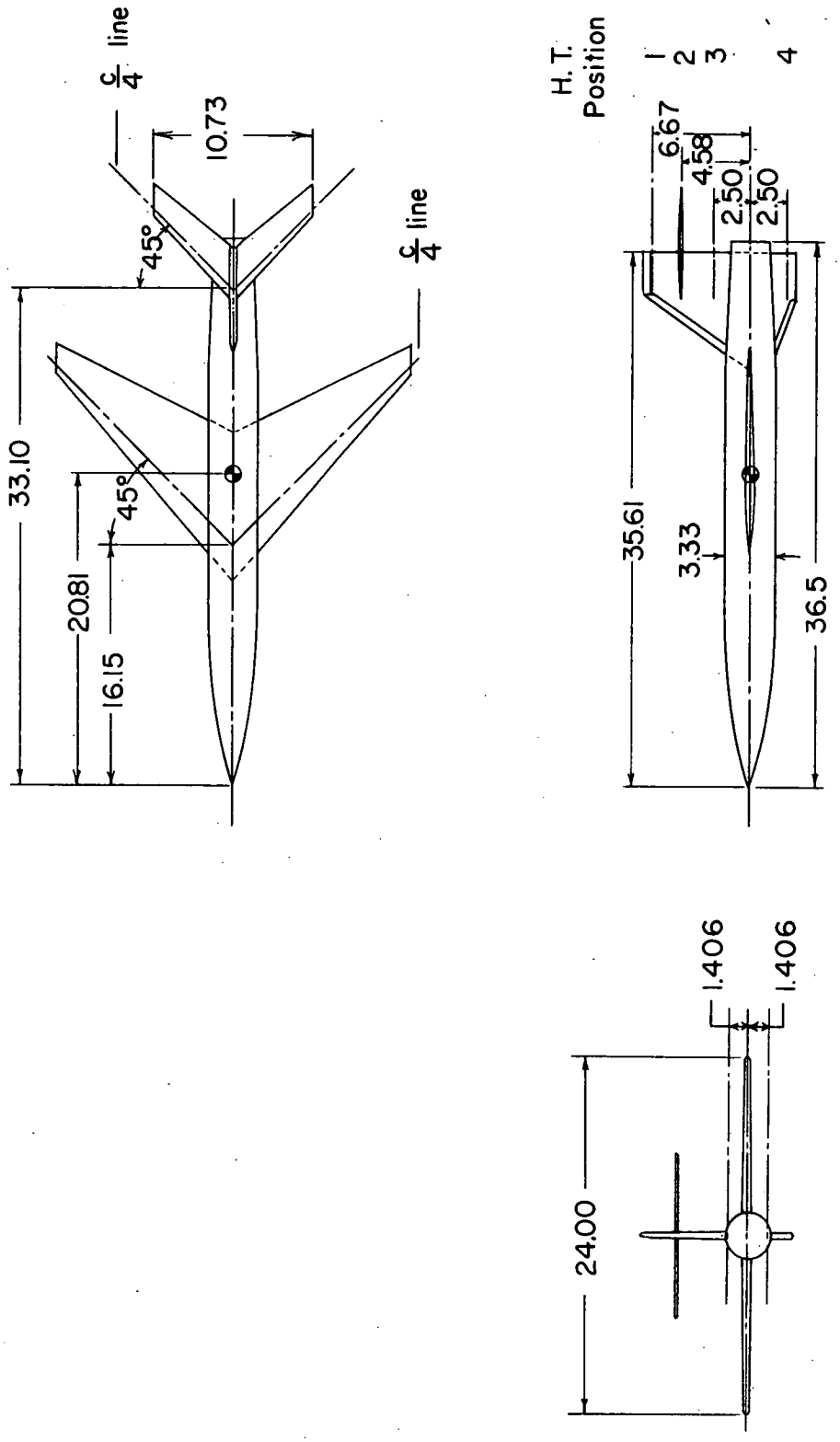

(a) Complete configuration.

Figure 2.- Details of model. All dimensions are in inches unless otherwise noted.

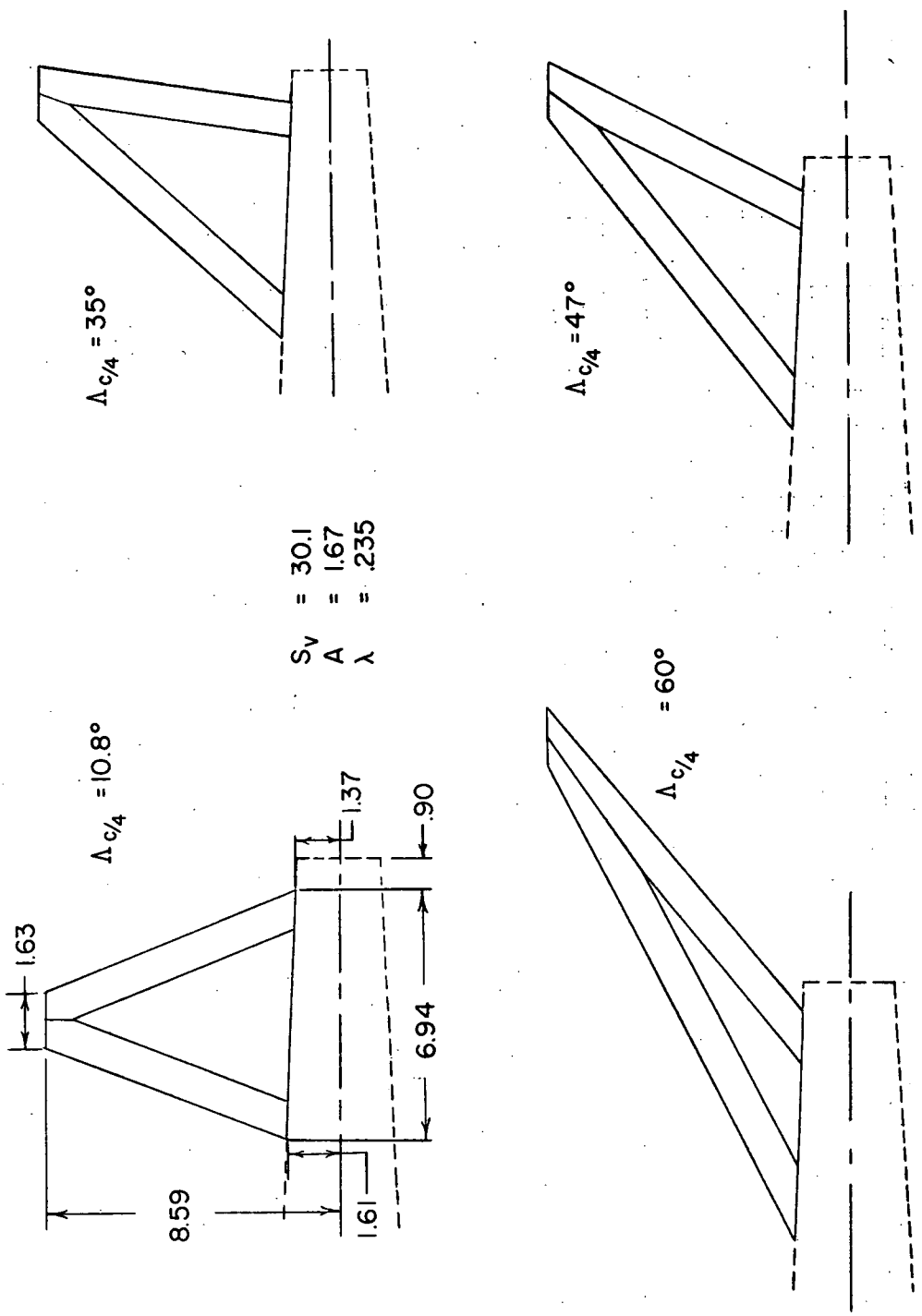

(b) Details of swept vertical tails.

Figure 2.- Concluded.

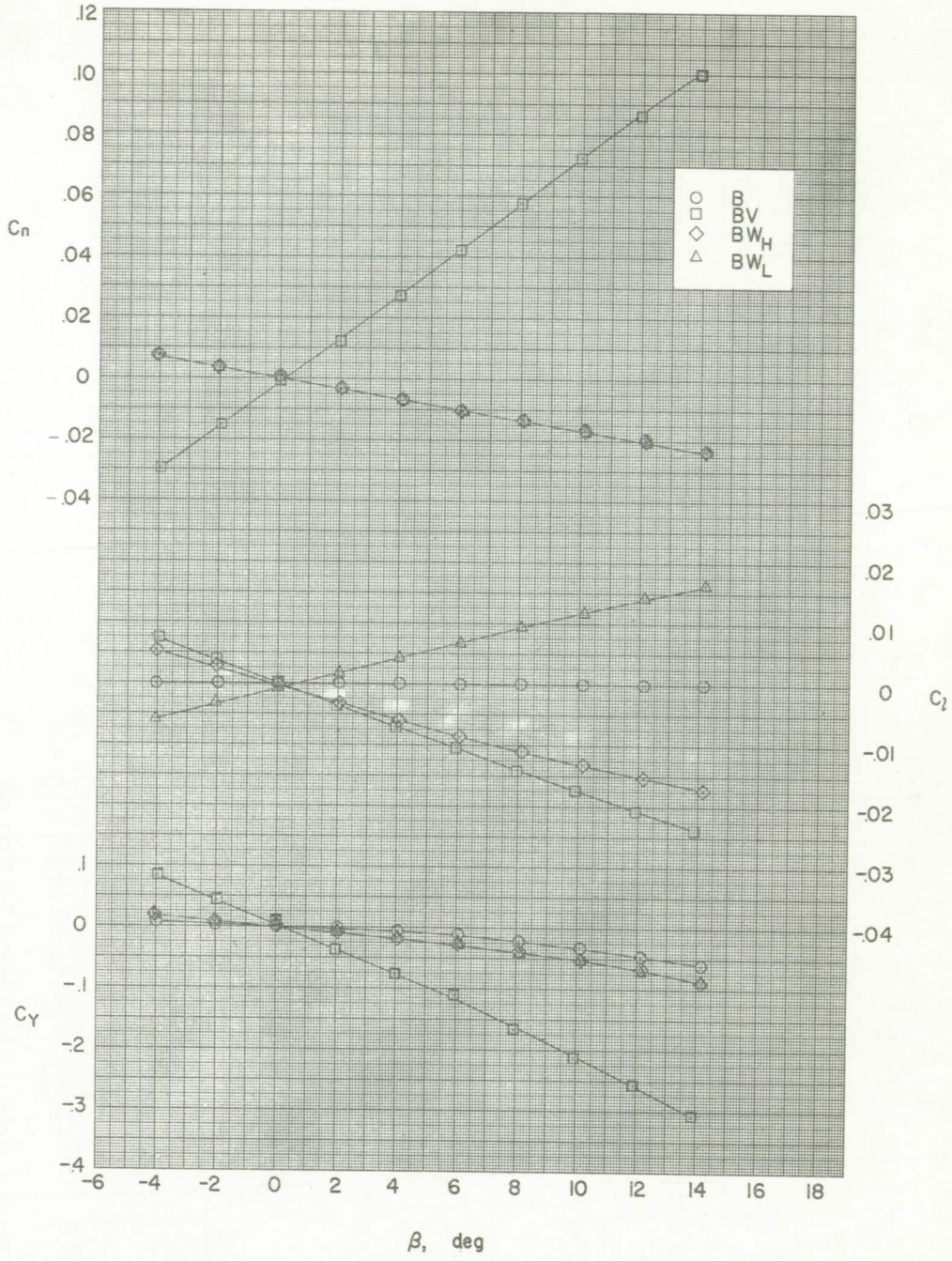

(a) $\alpha \approx 0^\circ$.

Figure 3.- Effect of component parts on aerodynamic characteristics in sideslip. M = 1.41.

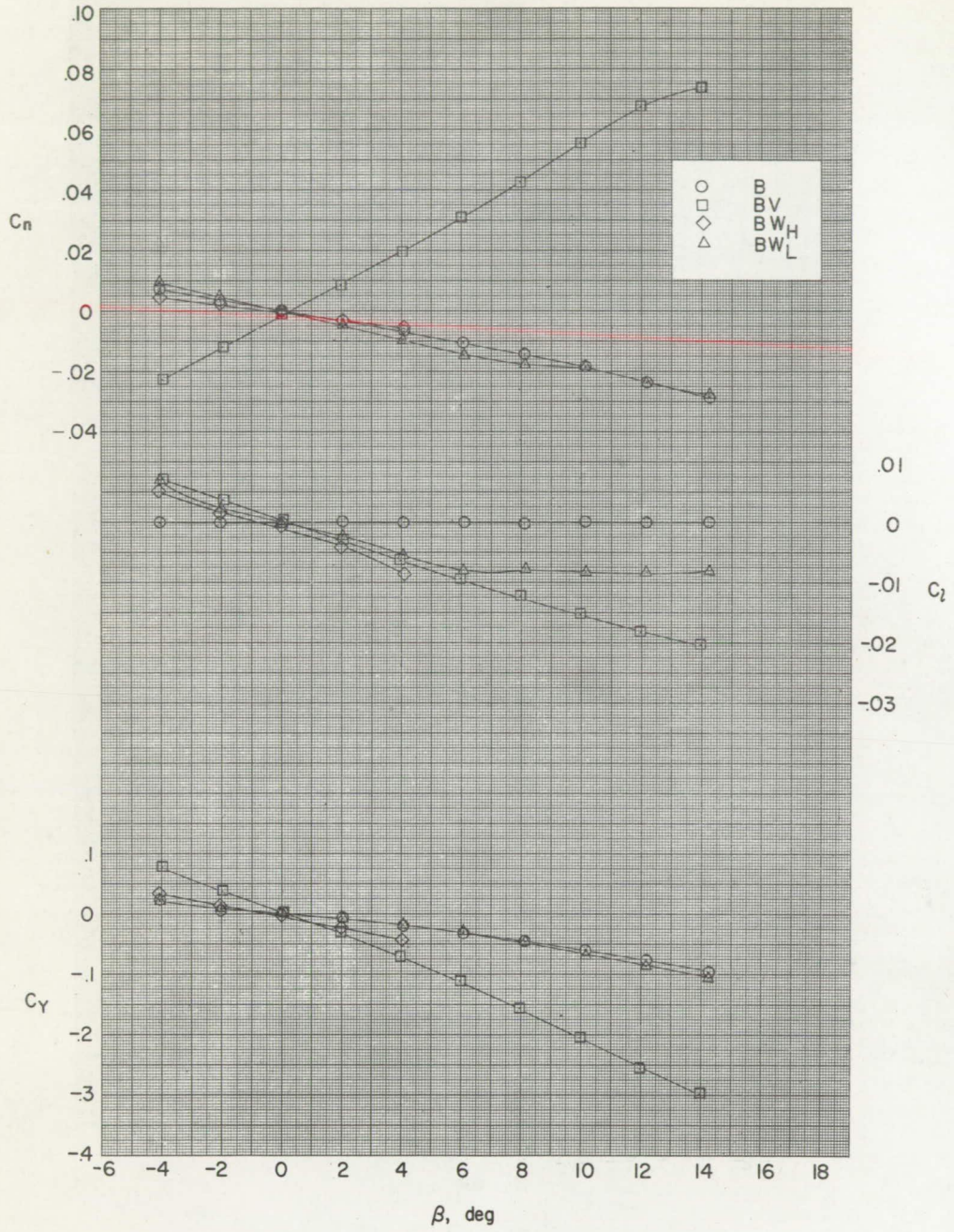

(b) $\alpha \approx 15.3^{\circ}$.

Figure 3.- Concluded.

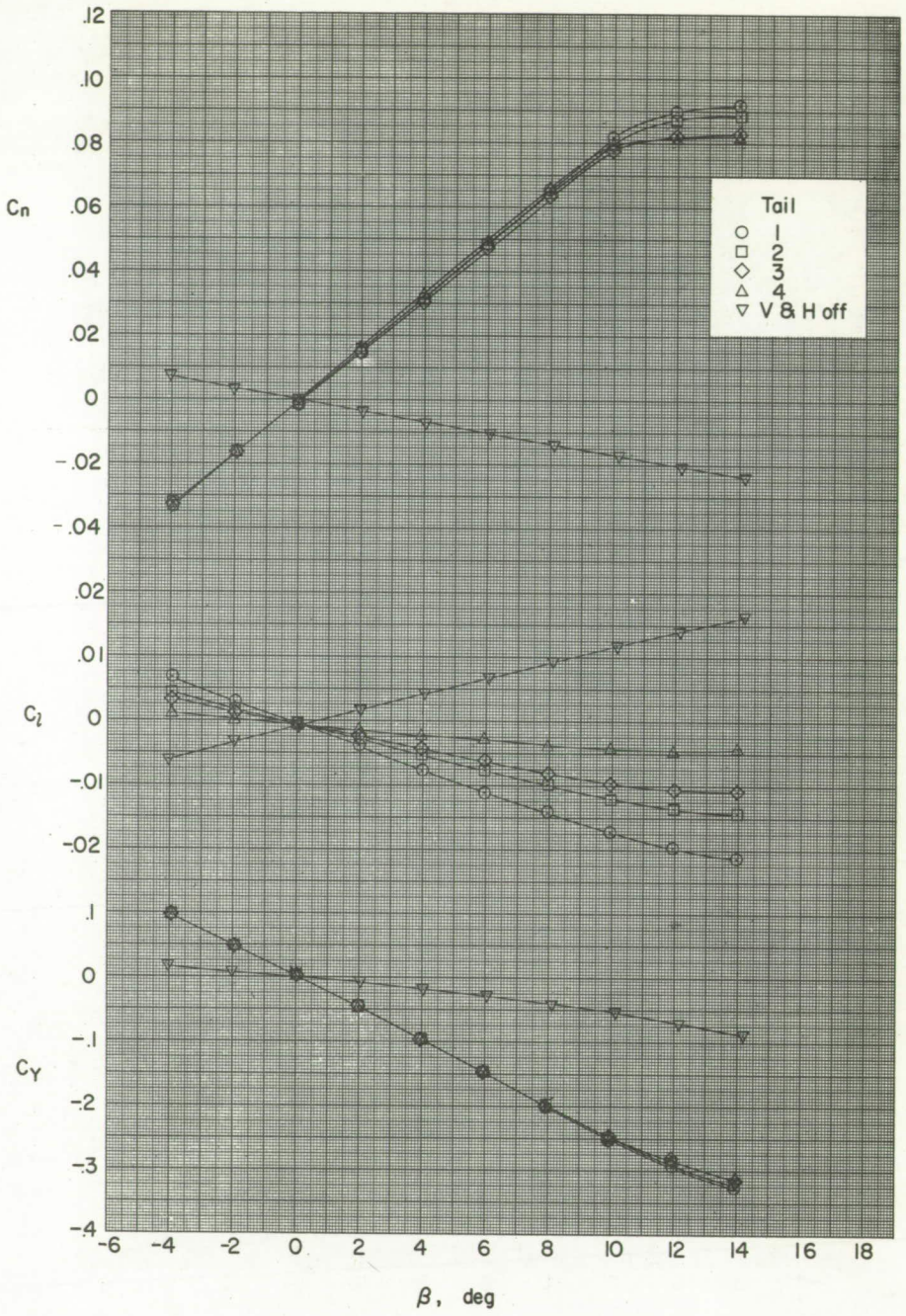

(a) $\alpha \approx 0^\circ$.

Figure 4.- Effect of horizontal-tail position on aerodynamic characteristics in sideslip for low-wing model. M = 1.41.

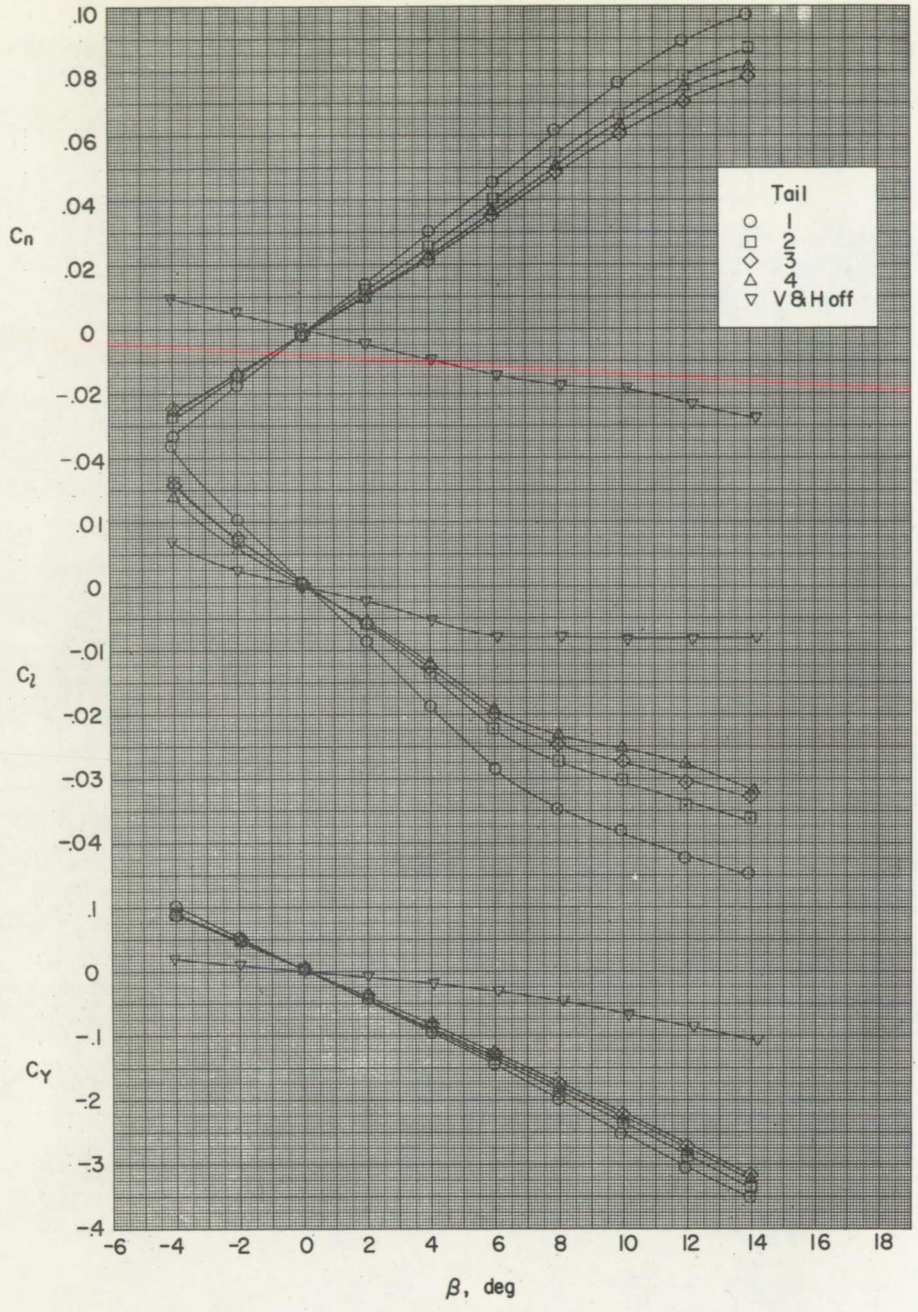

(b) $\alpha \approx 15.3^{\circ}$.

Figure 4.- Concluded.

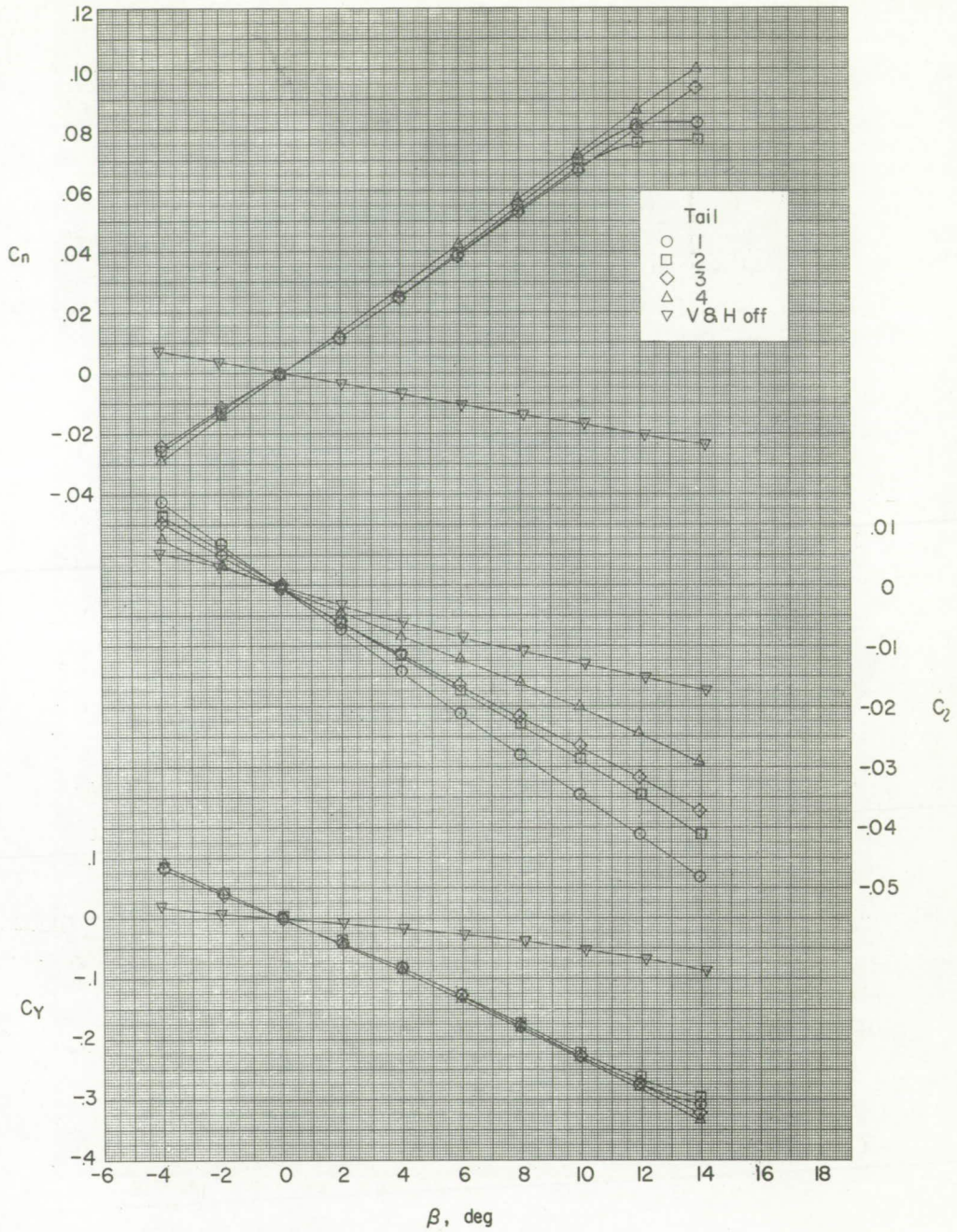

(a) $\alpha \approx 0^\circ$.

Figure 5.- Effect of horizontal-tail position on aerodynamic characteristics in sideslip for high-wing model. M = 1.41.

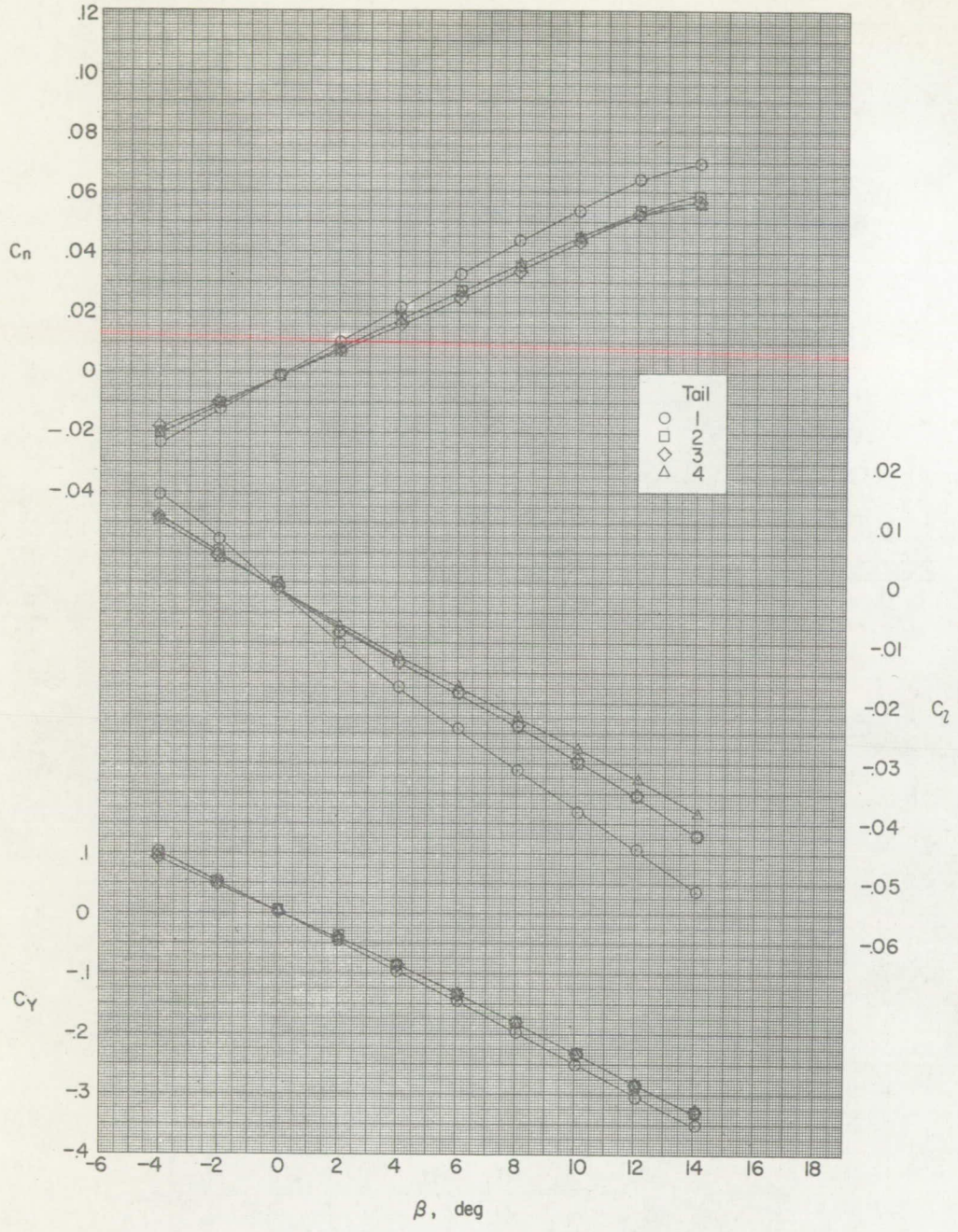

(b) $\alpha \approx 15.3^{\circ}$.

Figure 5.- Concluded.

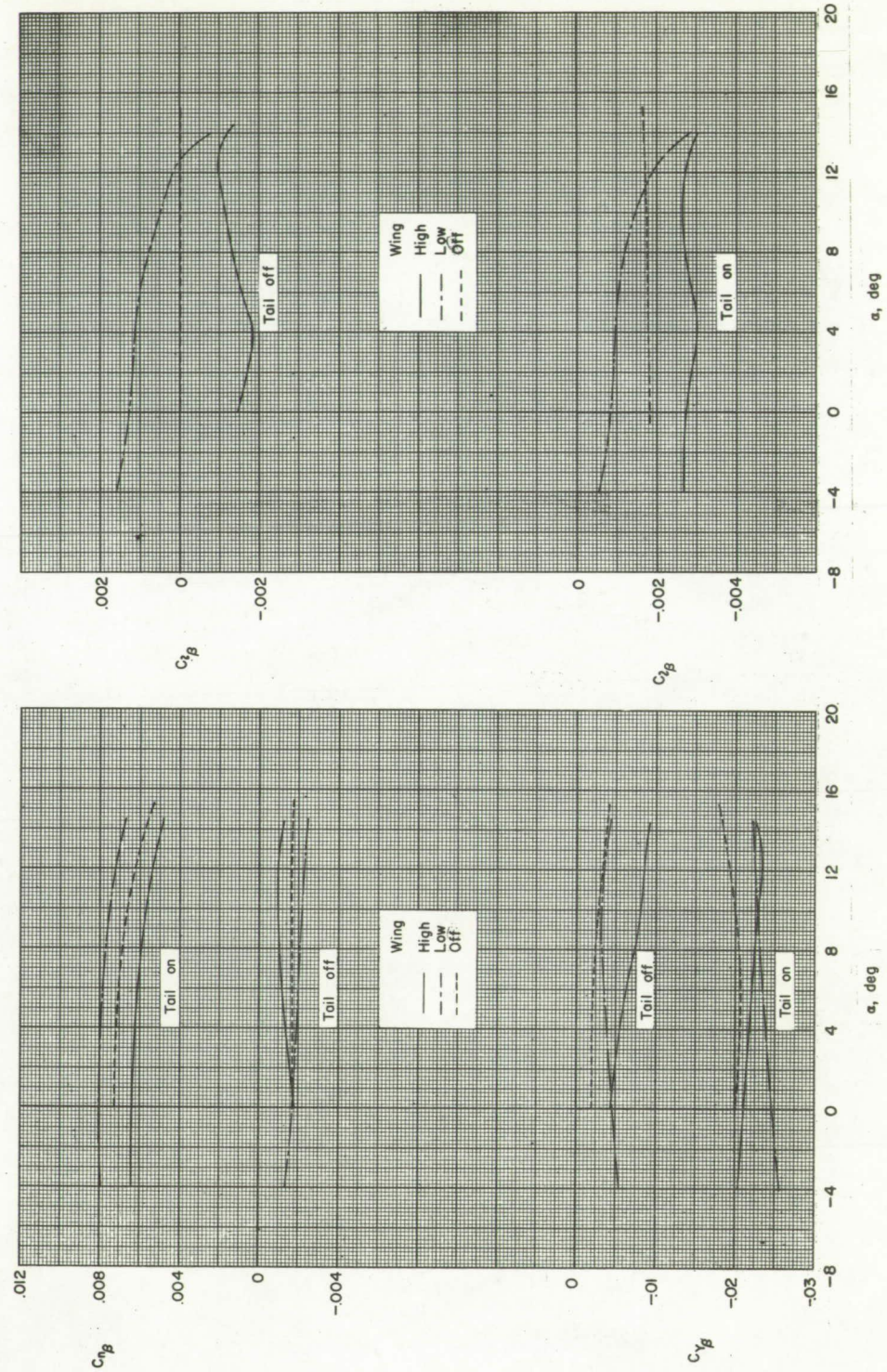

(a) M = 1.41.

Figure 6.- Effect of wing position on the aerodynamic characteristics in sideslip. Horizontal tail off.

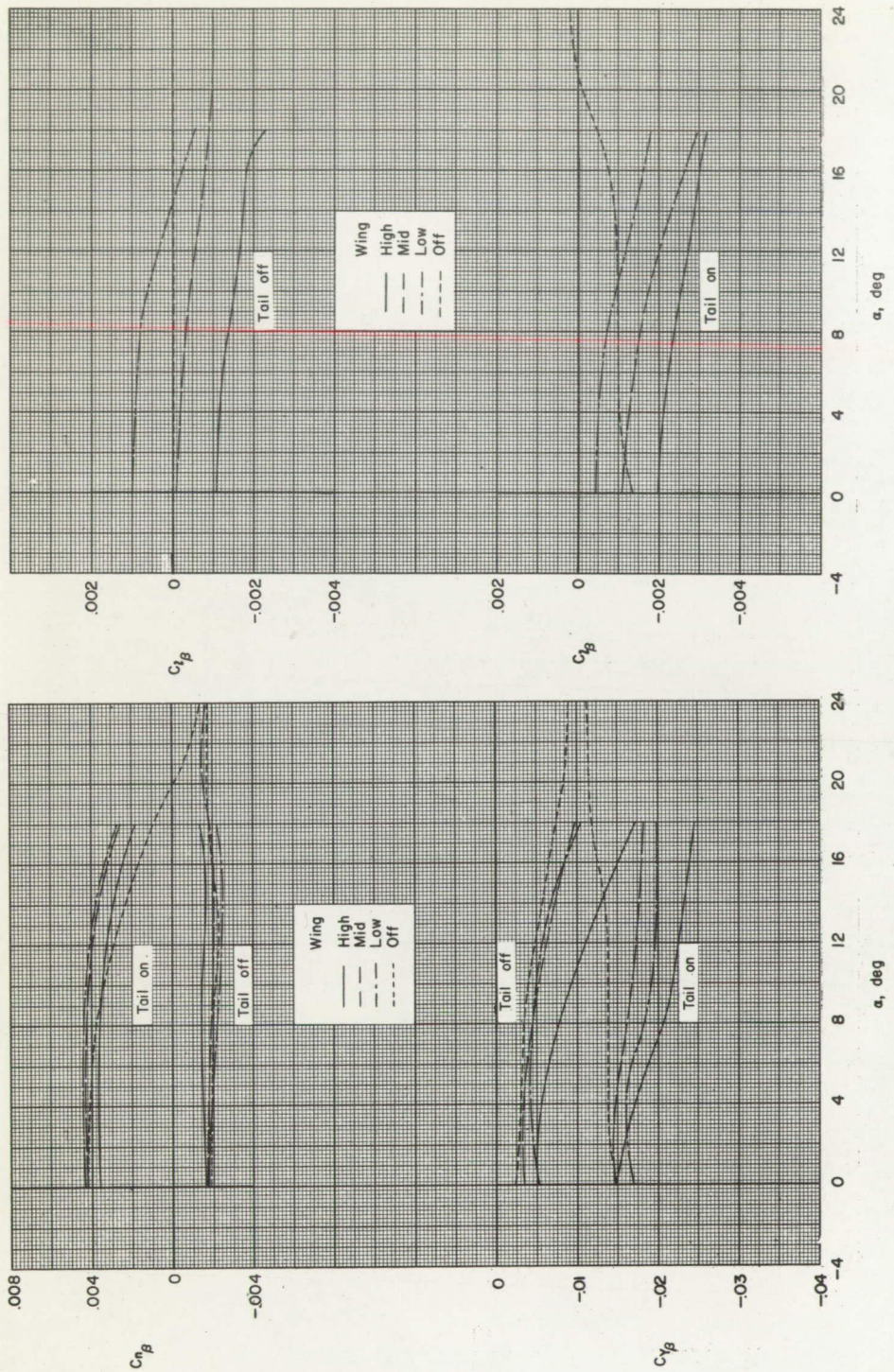

(b) M = 2.01.

Figure 6.- Concluded.

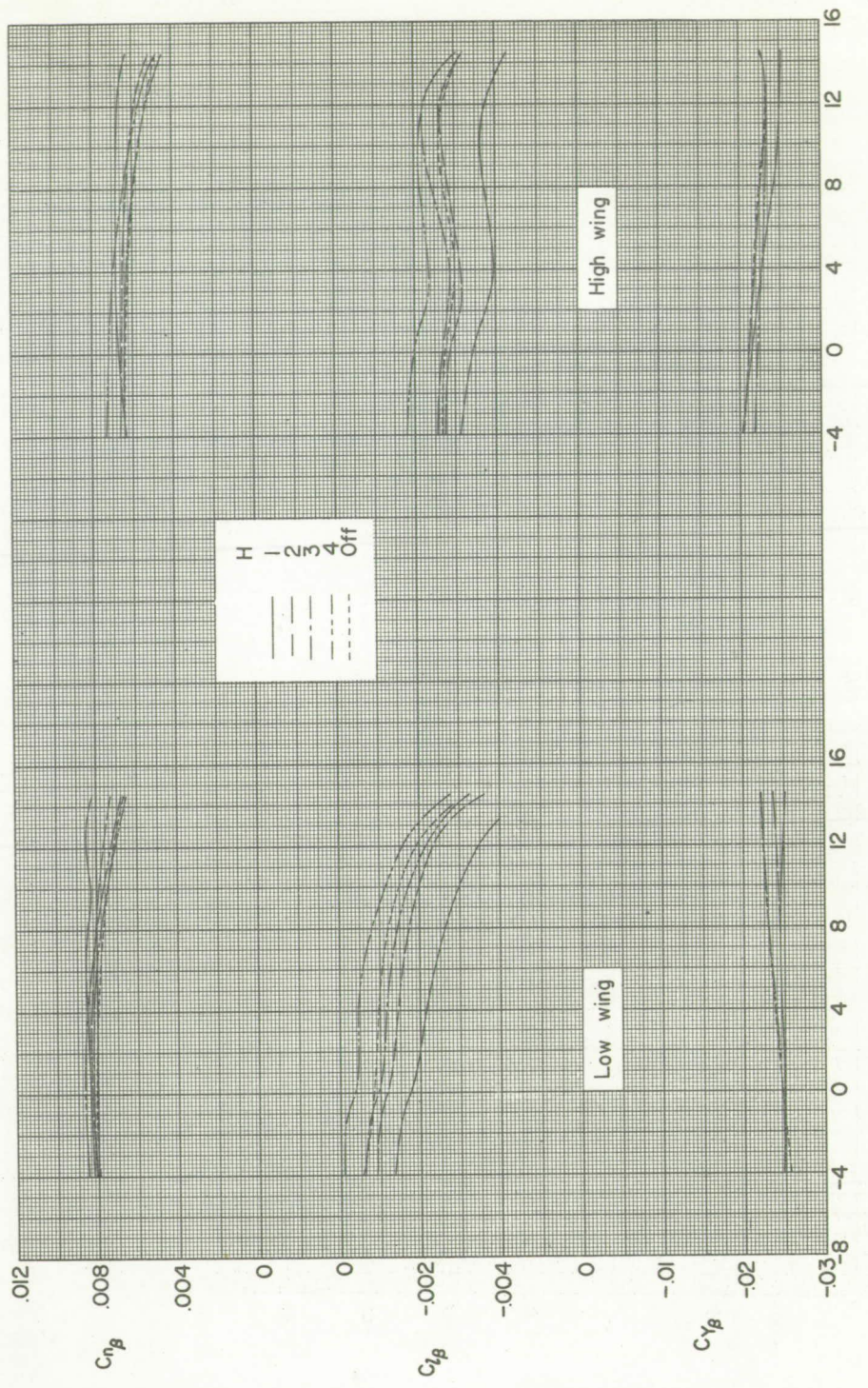

(a) M = 1.41.

Figure 7.- Effect of horizontal-tail position on the aerodynamic characteristics in sideslip for low- and high-wing models.

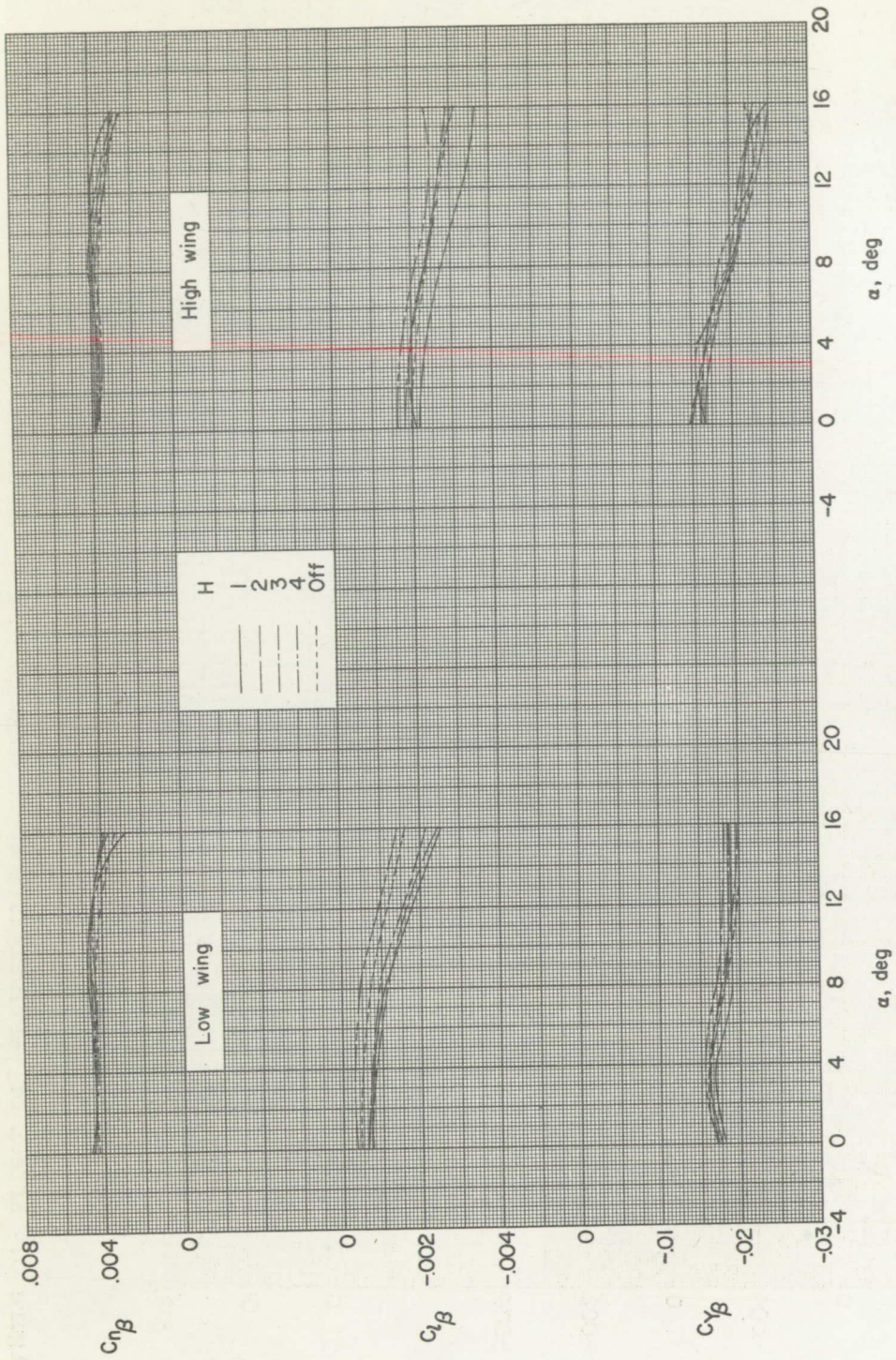

(b) M = 2.01

Figure 7.- Concluded.

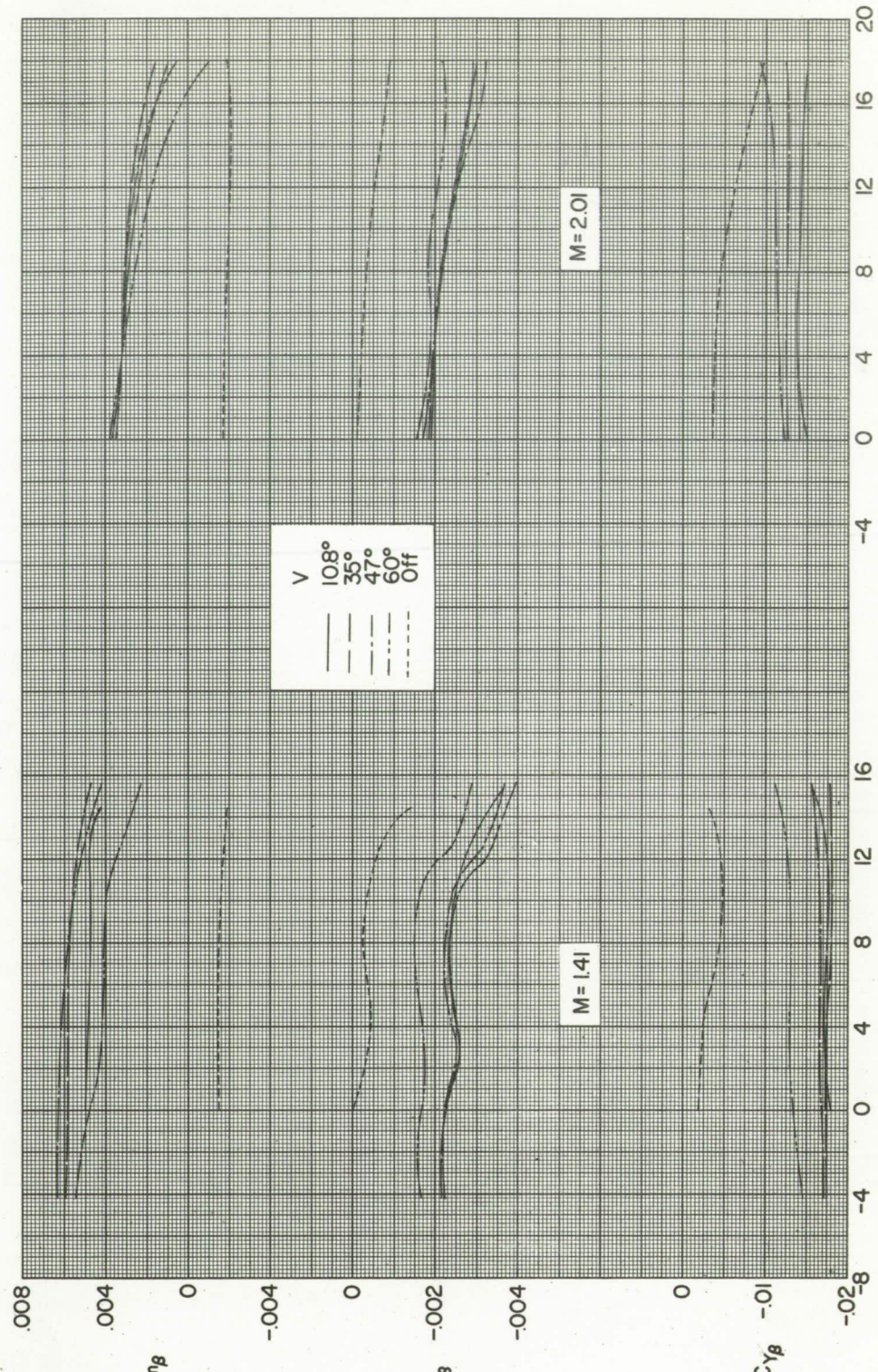

Figure 8.- Effect of vertical-tail sweep on aerodynamic characteristics in sideslip. Midwing position; no horizontal tail.

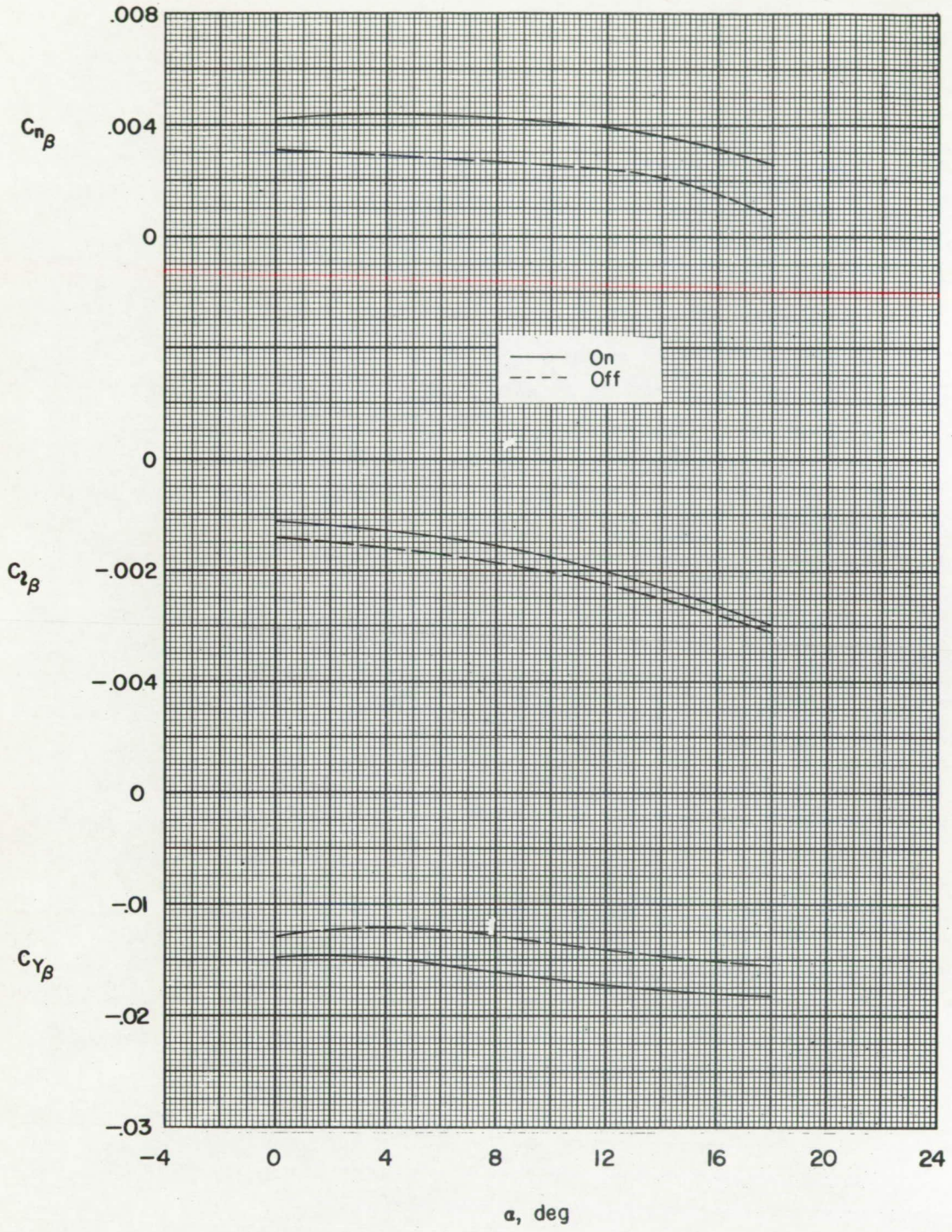

Figure 9.- Effect of ventral fin on the aerodynamic characteristics in sideslip. Midwing position; no horizontal tail; M = 2.01.